

Theory of high-order harmonic generation from molecules by intense laser pulses

This article has been downloaded from IOPscience. Please scroll down to see the full text article.

2008 J. Phys. B: At. Mol. Opt. Phys. 41 081002

(<http://iopscience.iop.org/0953-4075/41/8/081002>)

View [the table of contents for this issue](#), or go to the [journal homepage](#) for more

Download details:

IP Address: 38.107.179.212

The article was downloaded on 22/02/2012 at 07:11

Please note that [terms and conditions apply](#).

FAST TRACK COMMUNICATION

Theory of high-order harmonic generation from molecules by intense laser pulses

Anh-Thu Le¹, R Della Picca², P D Fainstein², D A Telnov³, M Lein⁴
and C D Lin¹

¹ J R Macdonald Laboratory, Department of Physics, Kanas State University, Manhattan, KS 66506, USA

² Centro Atomico Bariloche, Comisión Nacional de Energía Atómica, Avda E Bustillo 9500, 8400 Bariloche, Argentina

³ Department of Physics, St Petersburg State University, St Petersburg 198504, Russia

⁴ Institut für Physik and Center for Interdisciplinary Nanostructure Science and Technology, University of Kassel, Heinrich-Plett-Straße 40, 34132 Kassel, Germany

Received 15 February 2008

Published 3 April 2008

Online at stacks.iop.org/JPhysB/41/081002

Abstract

We show that high-order harmonics generated from molecules by intense laser pulses can be expressed as the product of a returning electron wave packet and the photo-recombination cross section where the electron wave packet can be obtained from the simple strong-field approximation (SFA) or from a companion atomic target. Using these wave packets but replacing the photo-recombination cross sections obtained from SFA or from the atomic target by the accurate cross sections from molecules, the resulting high-order harmonic spectra are shown to agree well with the benchmark results from direct numerical solution of the time-dependent Schrödinger equation, for the case of H_2^+ in laser fields. The result illustrates that these powerful theoretical tools can be used for obtaining high-order harmonic spectra from molecules. More importantly, the results imply that the photo-recombination cross section extracted from laser-induced high-order harmonic spectra can be used for time-resolved dynamic chemical imaging of transient molecules with temporal resolutions down to a few femtoseconds.

(Some figures in this article are in colour only in the electronic version)

High-order harmonic generation (HHG) is one of the most studied nonlinear phenomena in intense laser-matter interaction [1]. HHG is most easily understood using the three-step model [2–4]: first, the electron is released by tunnel ionization; second, it is accelerated by the oscillating electric field of the laser and later driven back to the target ion; and third, the electron recombines with the ion to emit a high-energy photon. A semiclassical formulation of the three-step model based on the strong-field approximation (SFA) is given by Lewenstein *et al* [4]. In this model (often called the Lewenstein model), the liberated continuum electron experiences the full effect from the laser field, but the effect

of the target potential is neglected. Despite this limitation, the Lewenstein model has been widely used for studying HHG from atoms and molecules, and for characterizing the nature of the harmonics generated. Since the continuum electron needs to come back to revisit the parent ion in order to emit radiation, the neglect of the electron-ion interaction in the SFA model is rather questionable. In the past few years, various efforts have been made to improve upon the SFA model, i.e., by including the Coulomb distortion [5–8] or by using the Ehrenfest theorem [9]. All of these improvements can still be considered insufficient since they fail to accurately include the scattering of the continuum electrons with the parent ions.

With moderate effort, direct numerical solution of the time-dependent Schrödinger equation (TDSE) for atomic targets can be accurately carried out, at least within the single active electron (SAE) approximation. The TDSE methods are computationally more demanding for molecular targets. Even for simplest diatomic molecules, one has to solve a three-dimensional time-dependent Schrödinger equation provided the molecular axis has an arbitrary orientation with respect to the polarization of the laser field. Such calculations require fast CPU and large memory computers and have been accomplished only recently [10–12]. In order to compare with experimental results, thus most of the existing calculations for HHG from molecules were carried out using the SFA model [13–15]. Based on the experience from high harmonics generated by atomic targets, such SFA model is not expected to offer accurate predictions. The lack of a reliable theory for describing HHG from molecules has prevented the possible exploitation of molecular structure using infrared laser pulses. This is unfortunate since it has been well recognized that infrared lasers have the potential for probing time-resolved molecular dynamics, with temporal resolutions down to sub-femtoseconds.

In view of the difficulty in solving the TDSE as a practical theoretical tool for predicting the nonlinear interactions between molecules with intense lasers, recently Le *et al* [16] and Morishita *et al* [17] have developed an alternative approach for calculating HHG and have tested the model for atomic targets. The theory is based on the three-step model but without the approximations that lead to the SFA (or the Lewenstein model). The HHG is viewed as resulting from the photo-recombination of the returning electrons generated by the laser pulses. The HHG yield is expressed as the product of a returning wave packet with the photo-recombination cross section. The shape of the wave packet has been shown to be largely independent of the targets for the same laser pulse and can thus be obtained from a reference atom or from the SFA. Thus, there are two ways to obtain HHG spectra without actually solving the TDSE. The first method is called SW-SFA model where the HHG spectra are obtained by replacing the dipole matrix element using scattering waves for the continuum electrons instead of the plane waves used in the SFA, but retaining the electron wave packet from the SFA. The other method is to compare the HHG spectra with another reference atom where the HHG spectra have been obtained by accurate calculations or by experiment. If the accurate photo-recombination cross sections for both the reference atom and the target are known, then the HHG spectra can be obtained from the HHG spectra of the other atom. The validity of the two methods have been established in Le *et al* [16] and Morishita *et al* [17] for atomic systems where the results from the models are compared to accurate results from the TDSE. While the model has been tested only for atoms so far, there is a general belief that the same models would apply to molecular targets also. In this communication, our goal is to apply the models to H_2^+ molecules where accurate HHG spectra have been calculated by solving the TDSE [10–12]. The results from this comparison confirm that the models indeed work well and the method can be extended further as a general tool for calculating HHG from molecular targets.

First let us be specific about the two methods for obtaining HHG spectra. The first method is called the scattering-wave-based strong-field approximation (SW-SFA) [16]. The HHG yield $S(\theta, \omega)$ for a molecule whose internuclear axis makes an alignment angle θ with respect to the laser polarization direction can be obtained from the SFA result $S^{\text{SFA}}(\theta, \omega)$ by

$$S(\theta, \omega) = \left| \frac{T(\theta, E)}{T^{\text{PWA}}(\theta, E)} \right|^2 S^{\text{SFA}}(\theta, \omega) \quad (1)$$

where T and T^{PWA} are the *exact* transition dipole matrix element and its plane-wave approximation (PWA), respectively. Here the electron energy E is related to the emitted photon energy ω by $E = k^2/2 = \omega - I_p$, with I_p being the ionization potential of the target (atomic units are used throughout the communication unless otherwise indicated). As only the ratio of the transition dipoles enters equation (1), one can formulate the SW-SFA model by using the above equation with the photoionization or its time-reversed process, i.e., the photo-recombination cross sections. In this communication we refer to the photoionization process, as it is more widely available theoretically and experimentally. Note that one can identify, up to some factor, $S^{\text{SFA}}/|T^{\text{PWA}}|^2$ as the flux of the returning electron, which we will call a ‘wave packet’. The returning electron that contributes most to the HHG is the one that propagates along the laser polarization direction. Therefore, the relevant differential cross section is for k that is parallel to the laser polarization axis, that is, for $\theta_k = 0$ and π . Note that for asymmetric molecules, the two contributions from $\theta_k = 0$ and π differ, in general.

Clearly, the formulation of the SW-SFA given in equation (1) is not unique. In fact, one can also use the ‘wave packet’ from a reference atom (i.e., atom with the same I_p as for the target). In other words, the HHG yield can also be written as

$$S(\theta, \omega) = \left| \frac{T(\theta, E)}{T^{\text{ref}}(E)} \right|^2 S^{\text{ref}}(\omega) \quad (2)$$

where the superscript ‘ref’ refers to the reference atom. We note that wave packets from reference atoms have been used before [18, 19]. In the following, we will check the validity of both models by comparing their predictions against the benchmark data. For the reference atom, we will use a scaled hydrogen with the effective nuclear charge chosen such that it has the same 1s binding energy as H_2^+ . The advantage of using the scaled hydrogen as a reference atom is that one can accurately and efficiently calculate both the HHG yield by solving the TDSE numerically and the exact photo-recombination cross section analytically. Experimentally, one can also replace the scaled atomic hydrogen with an atomic target of comparable ionization energy.

In this communication, we will focus only on the HHG component in the parallel polarization direction. The theoretical methods used to generate the data for the present study have all been given previously. The ‘benchmark’ HHG spectra of H_2^+ are calculated by solving the TDSE using the methods given in [10, 12]. The calculation of the transition dipole matrix elements are described in [20, 21] while the HHG calculated within the SFA is given in [13–15]. In terms

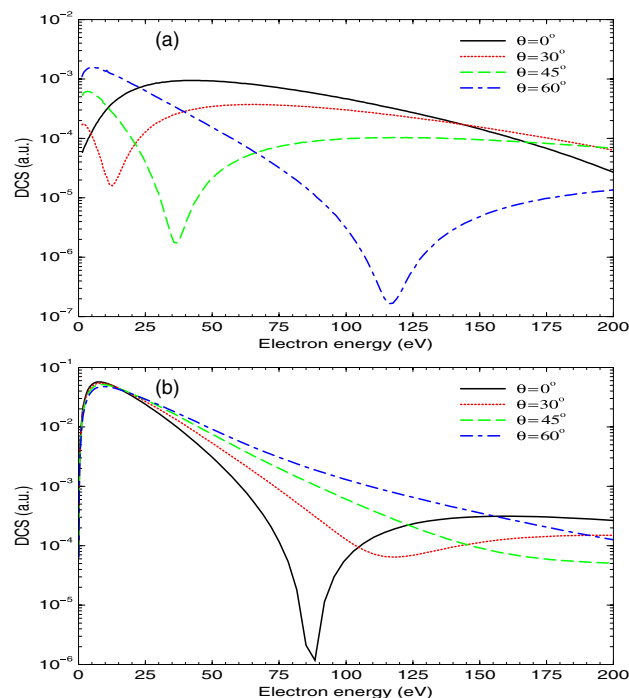


Figure 1. Comparison of the photoionization differential cross sections from the exact (i.e., with scattering wave) and the plane-wave approximation calculations, shown in (a) and (b), respectively, for alignment angles $\theta = 0^\circ, 30^\circ, 45^\circ$ and 60° .

of computational effort and thus the accuracy, the solution of the TDSE is the most demanding.

In figure 1(a) we show the photoionization differential cross sections (DCS) (electrons moving along the polarization axis), as functions of emitted electron energy, for H_2^+ at the equilibrium distance $R = 2.0$ au, alignment angles $\theta = 0^\circ, 30^\circ, 45^\circ$ and 60° . The data are shown for the energy range up to 200 eV, relevant to harmonic generation from typical infrared lasers. The noticeable features of these curves are the pronounced minima which move to the higher energies, as the alignment angle increases. The minimum positions are 12 eV, 36 eV and 117 eV, for $\theta = 30^\circ, 45^\circ$ and 60° , respectively. As we will show later, these minima are responsible for the interference minima, seen in the HHG spectra. The corresponding data obtained from the PWA are plotted in figure 1(b). Apart from the clear differences in the shape of these curves in comparison to the exact data, there are strong discrepancies in the positions of the minima. For $\theta = 30^\circ$, the minimum is shifted to higher energy as much as about 100 eV. For the two larger angles, the minima are not even seen within the energy range of the plot. That is the reason that the minima in the HHG spectra from SFA are shifted to much higher harmonic orders in comparison to the exact TDSE calculations, as observed by Kamta and Bandrauk [11] and by Chirila and Lein [22].

Next we compare the HHG spectra calculated using the different models with those obtained from the solution of the TDSE. In figures 2(a)–(d) we show the TDSE (solid red lines) and SFA (dashed black lines) results against those from using SW-SFA (solid blue lines) and with the wave packet from

scaled hydrogen (solid black lines), for $R = 2.0$ au and $\theta = 0^\circ, 30^\circ, 45^\circ$ and 60° . We use a laser pulse with a peak intensity of 3×10^{14} W cm $^{-2}$, wavelength of 800 nm and a 20-cycle duration with a sine-square envelope. The TDSE results for H_2^+ were obtained by using the method described in [12]. Here, we have normalized the data near the cut-off and only the odd harmonics are shown.

For $\theta = 0^\circ$ and 30° , one can see that the SFA results disagree greatly with the TDSE results. The improvements by the SW-SFA and with the wave packet from the scaled hydrogen are quite striking. Indeed, the results from both models reproduce quite well the overall shape of the spectra over the broad range down to H21, i.e., just above the ionization threshold ($I_p = 30$ eV). For $\theta = 30^\circ$, the minimum in both model calculations near H27 comes from the dip near $E = 12$ eV in the exact DCS (see figure 1(a)). This minimum is consistent with the TDSE data [12], although not clearly seen in figure 1(b). In fact, this is also consistent with the earlier results by Lein *et al* [10] and Kamta and Bandrauk [11]. For $\theta = 45^\circ$, the minimum in both of our model calculations is near H43, which also agrees well with the prediction from all the available TDSE results reported in [11] (see their table II) and [12]. Again, this minimum comes from the dip near 36 eV in the exact DCS. We note that the minima from our model calculations here tend to be more pronounced, compared to the TDSE results. The remaining discrepancies could be due to the limitation of our model or because of the possible lack of convergence in the TDSE results. Finally, for $\theta = 60^\circ$, we note that all the data, including the SFA, agree quite well with the TDSE results. This is not entirely surprising since the shape of the photoionization DCS for this angle from the PWA is fairly close to that of the exact DCS for the relevant electron energy range below 70 eV (see figures 1(a)–(b)).

It is important to emphasize that for each new alignment the returning wave packet from the SFA is calculated again, whereas the wave packet from scaled hydrogen is, of course, alignment independent. It has been shown [17, 16] that the shape of the wave packet largely depends only on the laser field (for systems with identical ionization potentials). Using scaled hydrogen, one therefore can get only the *shape* of the wave packet, as a function of energy. To get the absolute magnitude of the HHG spectra from the latter, one needs to multiply by a factor, which accounts for the alignment-dependent ionization yield. This can be done, for example, by using the molecular tunnelling ionization theory [23].

To better quantify the prediction of the SW-SFA model for different molecular alignments against the TDSE results, we show in figures 3(a) and (b) the selective harmonics, H25, H35, H45, H55 and H65, respectively, against the alignment angles. For convenience, the data were normalized to 1.0 at $\theta = 0^\circ$. Again, the general shape, as well as the minimum position for each harmonic, is in quite good agreement.

We now show a detailed comparison of the HHG spectra from different calculations in figure 4 for the alignment angle $\theta = 50^\circ$. Here we use a 10-cycle laser pulse with a peak intensity of 5×10^{14} W cm $^{-2}$ and wavelength of 780 nm, the same as has been used by Lein *et al* [10]. The pulse is turned

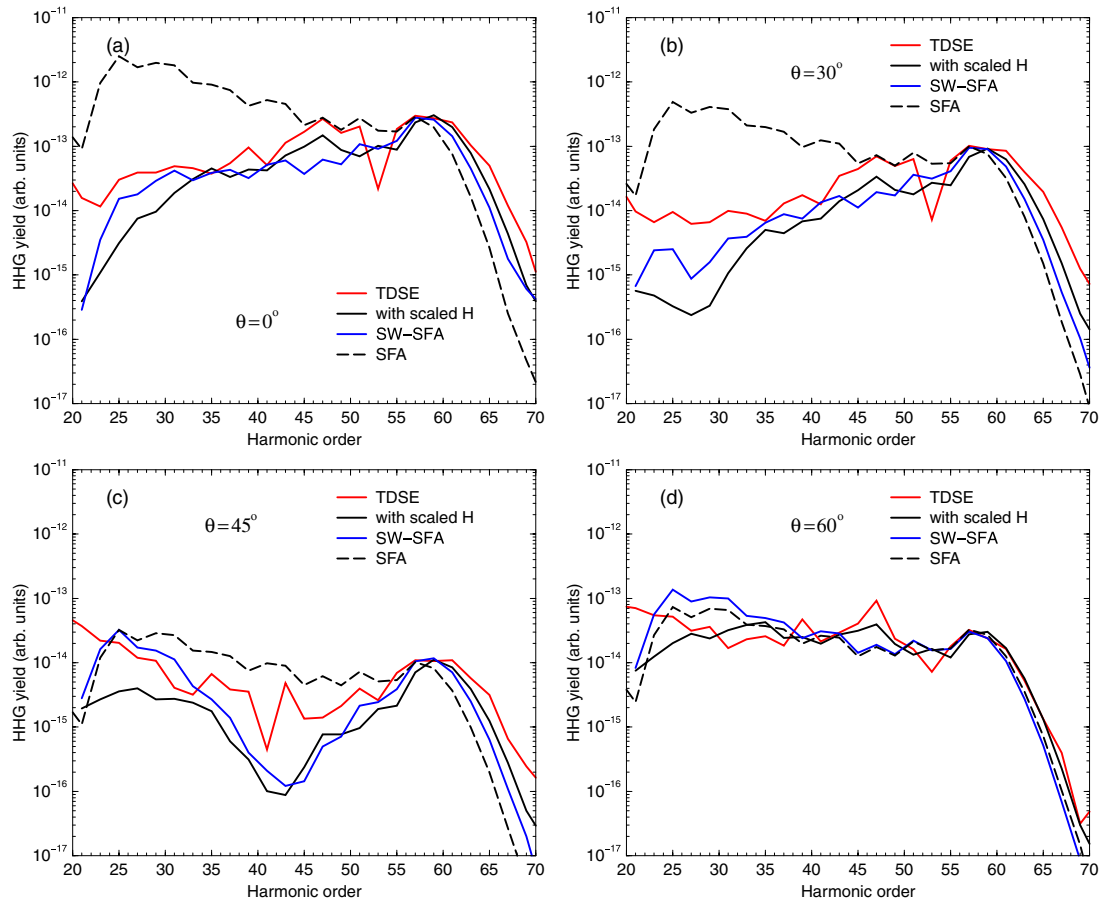


Figure 2. Comparison of the HHG spectra obtained from the TDSE (solid red lines), SFA (dashed lines), SW-SFA (solid blue lines) and with the use of scaled hydrogen atom (solid black lines) for the alignment angle $\theta = 0^\circ, 30^\circ, 45^\circ$ and 60° . A 20-cycle laser with a peak intensity of $3 \times 10^{14} \text{ W cm}^{-2}$ and wavelength of 800 nm is used.

on and off over three cycles and kept constant for four cycles. The TDSE results were obtained by the method described in [10]. For clarity, we have shifted the data vertically. Clearly, the SW-SFA data (blue line) are in quite good agreement with the TDSE results (red line). The results from our model using the wave packet calculated by solving the TDSE equation for scaled hydrogen (black line) agree even better with the TDSE results. In particular, the minimum near H55, indicated by an arrow in the figure, is well reproduced by both model calculations.

In recent years, the ‘interference minima’ in the HHG spectra from molecular targets have been widely discussed in the literature [14, 24–26]. As shown by Lein *et al* [27], the minimum positions in HHG spectra from the TDSE for H_2^+ with $R = 1.8, 2.0$ and 2.5 au agree quite well with the two-emitter model [24, 27]. Specifically, the minima satisfy the relation $R \cos(\theta) = \lambda^{\text{eff}}/2$, where λ^{eff} is the ‘effective’ wavelength of the continuum electron defined such that the ‘effective’ wave vector is $k^{\text{eff}} = \sqrt{2\omega}$, with ω being the energy of the emitted photon. In other words, the ‘effective’ energy is shifted by I_p with respect to the usual relation, i.e., $k = \sqrt{2(\omega - I_p)}$.

According to the two models presented here, the minima in HHG are attributed to the minima in the photoionization DCS. In figure 5, the projected internuclear separation

$R \cos(\theta)$ is plotted versus the ‘effective’ electron wavelength at the minima in the photoionization DCS. The data were obtained for $R = 1.8, 2.0, 2.5, 3.0$ and 4.0 au and for alignment angles $\theta = 30^\circ, 40^\circ, 50^\circ, 60^\circ$ and 70° . The results are indeed scattered nicely around $R \cos(\theta) = \lambda^{\text{eff}}/2$, shown as the dashed line, for small λ^{eff} and tend to lie above it for $\lambda^{\text{eff}} > 3.5$ au. This is consistent with the results from the numerical solution of the TDSE by Lein *et al* [27] (see their figure 3). This result demonstrates that the minima in the HHG spectra from H_2^+ are fully and accurately reproducible by the minima in the photoionization cross sections and hence, by the SW-SFA model, for other internuclear distances as well. We note in this connection that an analysis of the recombination cross sections in relation to the minima positions in the HHG spectra from H_2 and N_2 has been reported recently by Zimmermann *et al* [28].

In this communication, we have shown that harmonic generation from H_2^+ molecule can be factored out into the product of a returning electron wave packet with the photo-recombination cross section. The wave packet can be extracted from the SFA model or from HHG generated by atoms with similar ionization potential. Using either wave packet, but replacing the photo-recombination cross section of either case by the accurate cross section of the molecule, we show that the

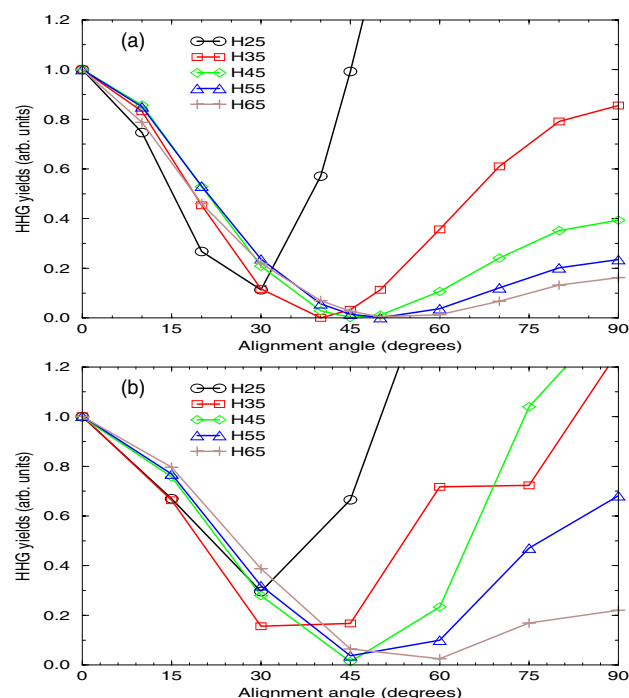


Figure 3. Alignment dependence of some selected harmonics from the SW-SFA (a) and the TDSE (b).

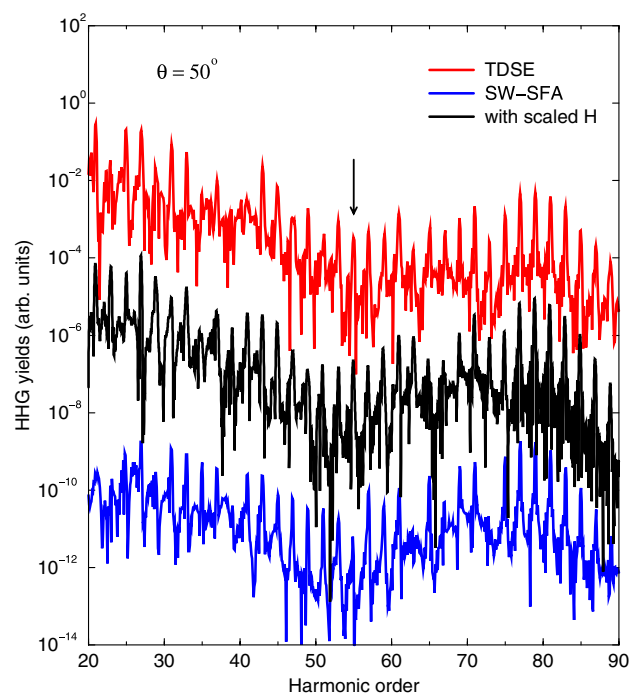


Figure 4. Comparison of the HHG spectra obtained from the TDSE (red line), SW-SFA (blue line) and with the use of the returning wave packet from scaled hydrogen (black line), for alignment angle $\theta = 50^\circ$. The data have been shifted vertically to show the details. A laser pulse with peak intensity of $5 \times 10^{14} \text{ W cm}^{-2}$ and wavelength of 780 nm is used. The pulse is turned on and off over three cycles and kept constant for four cycles. The arrow indicates the position of the interference minimum.

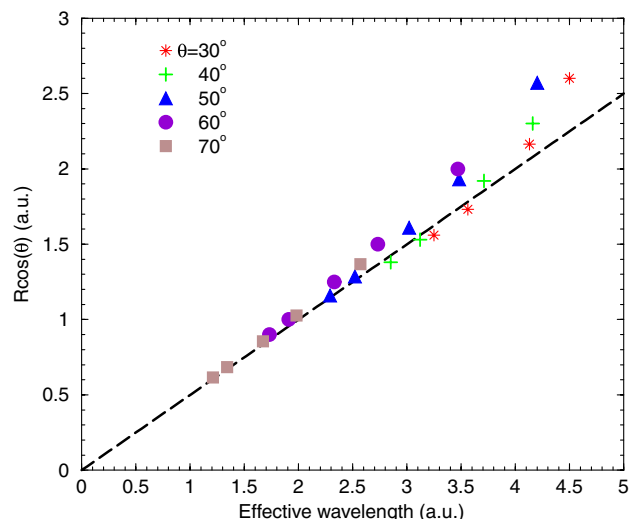


Figure 5. Projected internuclear separation versus ‘effective’ electron wavelength at the minima in the *exact* photoionization cross sections. Data were obtained with $R = 1.8, 2.0, 2.5, 3.0$ and 4.0 au, and for different alignment angles as shown in the labels. Note that we have used the ‘effective’ wavelength according to Lein *et al* [27], see the text.

resulting HHG spectra compared favourably with those from solving the TDSE. Similar conclusions have been reached for atomic targets recently [16, 17]. The models have been tested using different laser parameters and for different internuclear distances, and we expect the models to work well for molecules in general. Since photoionization (or photo-recombination) is a linear process, it is intrinsically much easier to treat theoretically than the nonlinear laser–molecule interaction. While accurate calculations of molecular photoionization DCS are by no means trivial, sophisticated packages have been developed [29–31] over the years. Furthermore, for the purpose of obtaining HHG spectra for molecules in the intense laser pulses, high-precision cross sections in a narrow energy region such as those measured with synchrotron radiation are not needed. Instead, moderately accurate results over a broad range of energy such as those based on the one-electron model developed by Tonzani [32] are likely adequate.

The significance of the present result is not limited to a workable theory for HHG from molecules. Most importantly, the results suggest that it is possible to extract photoionization cross sections over a broad energy range from the measured HHG spectra which may then be used to unravel the structure of the target molecule. Since infrared lasers with sub-ten femtoseconds are already widely available, high-order harmonics generated from molecules undergoing transformation may then be used to extract the structure of the transient molecules at different time delays. The potential of using HHG from molecules for time-resolved chemical imaging appears quite promising.

Acknowledgments

This work was supported in part by Chemical Sciences, Geosciences and Biosciences Division, Office of Basic

Energy Sciences, Office of Science and US Department of Energy. ML acknowledges support from Deutsche Forschungsgemeinschaft.

References

- [1] Brabec T and Krausz F 2000 *Rev. Mod. Phys.* **72** 545
- [2] Kulander K C, Schafer K J and Krause J L 1993 *Super Intense Laser-Atom Physics NATO Advanced Study Institute Series* (New York: Plenum) p 95
- [3] Corkum P B 1993 *Phys. Rev. Lett.* **71** 1994
- [4] Lewenstein M, Balcou Ph, Ivanov M Yu, L'Huillier A and Corkum P B 1994 *Phys. Rev. A* **49** 2117
- [5] Ivanov M Yu, Brabec T and Burnett N 1996 *Phys. Rev. A* **54** 742
- [6] Kaminski J Z and Ehlötzky F 1996 *Phys. Rev. A* **54** 3678
- [7] Ciappina M F, Chirila C C and Lein M 2007 *Phys. Rev. A* **75** 043405
- [8] Smirnova O, Mouritzen A S, Patchkovskii S and Ivanov M Yu 2007 *J. Phys. B: At. Mol. Opt. Phys.* **40** F197
- [9] Gordon A and Kartner F X 2005 *Phys. Rev. Lett.* **95** 223901
- [10] Lein M, Corso P P, Marangos J P and Knight P L 2003 *Phys. Rev. A* **67** 023819
- [11] Kamta G L and Bandrauk A D 2005 *Phys. Rev. A* **71** 053407
- [12] Telnov D A and Chu S I 2007 *Phys. Rev. A* **76** 043412
- [13] Zhou X X, Tong X M, Zhao Z X and Lin C D 2005 *Phys. Rev. A* **71** 061801
- [14] Le A T, Tong X M and Lin C D 2006 *Phys. Rev. A* **73** 041402
- [15] Le V H, Le A T, Xie R H and Lin C D 2007 *Phys. Rev. A* **76** 013414
- [16] Le A T, Morishita T and Lin C D 2008 *Phys. Rev. Lett.*, submitted (arXiv: 0712.3577v1)
- [17] Morishita T, Le A T, Chen Z and Lin C D 2008 *Phys. Rev. Lett.* **100** 013903
- [18] Itatani J, Levesque J, Zeidler D, Niikura H, Pepin H, Kieffer J C, Corkum P B and Villeneuve D M 2004 *Nature* **432** 867
- [19] Levesque J, Zeidler D, Marangos J P, Corkum P B and Villeneuve D M 2007 *Phys. Rev. Lett.* **98** 183903
- [20] Della Picca R, Fainstein P D, Martiarena M L and Dubois A 2006 *J. Phys. B: At. Mol. Opt. Phys.* **39** 473
- [21] Della Picca R, Fainstein P D, Martiarena M L and Dubois A 2007 *Phys. Rev. A* **75** 032710
- [22] Chirila C C and Lein M 2007 *J. Mod. Opt.* **54** 1039
- [23] Tong X M, Zhao Z and Lin C D 2002 *Phys. Rev. A* **66** 033402
- [24] Lein M, Hay N, Velotta R, Marangos J P and Knight P L 2002 *Phys. Rev. Lett.* **88** 183903
- [25] Kanai T, Minemoto S and Sakai H 2005 *Nature (London)* **435** 470
- [26] Vozzi C, *et al* 2005 *Phys. Rev. Lett.* **95** 153902
- [27] Lein M, Hay N, Velotta R, Marangos J P and Knight P L 2002 *Phys. Rev. A* **66** 023805
- [28] Zimmermann B, Lein M and Rost J M 2005 *Phys. Rev. A* **71** 033401
- [29] Huo W M and Gianturco F A 1995 *Computational Methods for Electron-Molecule Collisions* (New York: Plenum)
- [30] Lucchese R R, Lafosse A, Brenot J C, Guyon P M, Houver J C, Lebech M, Raseev G and Doweck D 2002 *Phys. Rev. A* **65** 020702
- [31] Cherepkov N A and Raseev G 1995 *J. Chem. Phys.* **103** 8238
- [32] Tonzani S 2007 *Comput. Phys. Commun.* **176** 146